Supplementary Information

Supplementary table 1: Further information of speleothem entities that were not analysed as a part of the main manuscript since they only partially cover Terminations or have lower resolution or U-Th dates with larger errors than the records used in the main manuscript. Cave site locations are plotted in Supp. Fig. 1 and time series plots are in Supp. Fig. 2. Some data from the main manuscript are included in the table and plots to enable comparison.

region	site name	latitude	longitude	elevation (m)	entity name	age model	data source	citation	primary interpretation	secondary interpretation	comments
South Europe	Corchia	43.9833	10.2167	840	CC-5_2018	SISAL-Bchron	SISAL v3	Tzedakis et al., 2018	rainfall amount	source water composition	
	Corchia	43.9833	10.2167	840	CC-1_2018	SISAL-copRa	SISAL v3	Tzedakis et al., 2017	rainfall amount	source water composition	
	Soreq	31.7558	35.0226	400	Soreq_composite (green)	author-linear between dates	SISAL v3	Bar-Matthews et al., 2003	rainfall amount	source water composition	composite includes stalactites;
	Jerusalem West	31.7833	35.15	700	AF12 (blue)	author-polynomial fit	SISAL v3	Frumkin et al., 1999	source water composition	change in moisture transport trajectory and linked seasonality	age reversals beyond 100k; calcite precipitation T and ice volume source composition
	La Vallina	43.4100	-4.8067	70	Garth	author-mixed Bchron	SISAL v3	Stoll et al., 2022	source water composition	temperature dependency of meteoric precipitation	confocal band counting
	Villars	45.43	0.78	175	Vil-car1	author-linear between dates	SISAL v3	Wainer et al., 2011	cave air temperature	disequilibrium	flowstone; authors flag possible detrital contamination and U-leaching giving older ages,

North Europe	Abaliget	46.1333	18.1167	209	ABA_1	author-StalAge	SISAL v3	Koltai et al., 2017	temperature dependency of meteoric precipitation	source water composition	flowstone; author generated age model uses both cores to create master chronology
	Schneckenloch	47.4333	9.8667	1285	SCH-5	SISAL-copRa	SISAL v3	Moseley et al., 2015	temperature dependency of meteoric precipitation	change in moisture transport trajectory	
	Sieben Hengste	46.75	7.81	1955	7H-12	author-StalAge	SISAL v3	Luetscher et al., 2021	temperature dependency of meteoric precipitation	change in moisture transport trajectory	
	Neotektonik	46.7833	8.2666	1700	M37-1-16A	author-OxCal	SISAL v3	Wilcox et al., 2020			paper focused on fluid inclusions, no $\delta^{18}O$ interpretations provided; no reported hiatus
North America	Lehman caves	39.01	-114.22	2080	LMC-14	SISAL-copRa	SISAL v3	Lachniet et al., 2014	temperature dependency of meteoric precipitation	change in moisture source latitude	
					LMC-21	SISAL-copRa	SISAL v3	Lachniet et al., 2014	temperature dependency of meteoric precipitation	change in moisture source latitude	
					LC-2	SISAL-Bchron	SISAL v3	Shakun et al., 2011			

	Devils Hole	36.4254	-116.2915	719	DH2-D	author-OxCal	SISAL v3	Moseley et al., 2016	temperature dependency of meteoric precipitation	change in seasonality	sub-aqueous calcite; shallowest core with least 230Th effect and youngest chronologies
EASM	Dongge	25.2833	108.0833	680	D4_2005_Kelly	author-unknown	SISAL v3	Kelly et al., 2006	change in seasonality	upstream rainout	
	Sanbao	31.667	110.4333	1900	SB11	sisal-copRa	SISAL v3	Cheng et al., 2016b	upstream rainout	change in seasonality	
					SB23	sisal-copRa	SISAL v3	Cheng et al., 2016b	upstream rainout	change in seasonality	
					SB25-2	sisal-copRa	SISAL v3	Cheng et al., 2016b	upstream rainout	change in seasonality	
					SB41	sisal-copRa	SISAL v3	Cheng et al., 2016b	upstream rainout	change in seasonality	
South Europe	Sofular	41.4167	31.9333	440	SO-4	SISAL-Bchron	SISAL v3	Badertscher et al., 2011	source water composition		more negative from Caspian Sea with melt waters, more positive from Mediterranean
	Crovassa Azzurra	39.28	8.48	410	CA	author-linear between dates	SISAL v3	Columbu et al., 2019	rainfall amount	change in moisture source	flowstone; mixed mineralogy -aragonite with some calcite
	Peqiin cave	32.58	35.19	650	PEK_composite	author-unknown	SISAL v3	Bar-Matthews et al., 2003	rainfall amount	source water composition	composite includes stalactites

	Ejulve	40.76	-0.59	1240	ARTEMISA	author-StalAge and other	SISAL v3	Pérez-Mejías et al., 2017	temperature change	source water composition	record focuses on $\delta^{13}C$ as proxy for dry conditions
Central Asia	Kesang	42.87	81.75	2000	KS06-A	SISAL-copRa	SISAL v3	Cheng et al., 2016a	large-scale circulation and supra-regional climate	change in moisture transport trajectory and linked seasonality	temperature effect on calcite precipitation
	Kesang	42.87	81.75	2000	KS08-1	SISAL-copRa	SISAL v3	Cheng et al., 2016a	large-scale circulation and supra-regional climate	change in moisture transport trajectory and linked seasonality	temperature effect on calcite precipitation
ISM	Xiaobailong	24.2	103.36	1500	XBL-26	SISAL-copRa	SISAL v3	Cai et al., 2015	rainfall amount		
	Bittoo	30.7903	77.7764	3000	BT-9	sisal-Bchron	SISAL v3	Kathayat et al., 2016	large-scale circulation, upstream changes, moisture transport history		

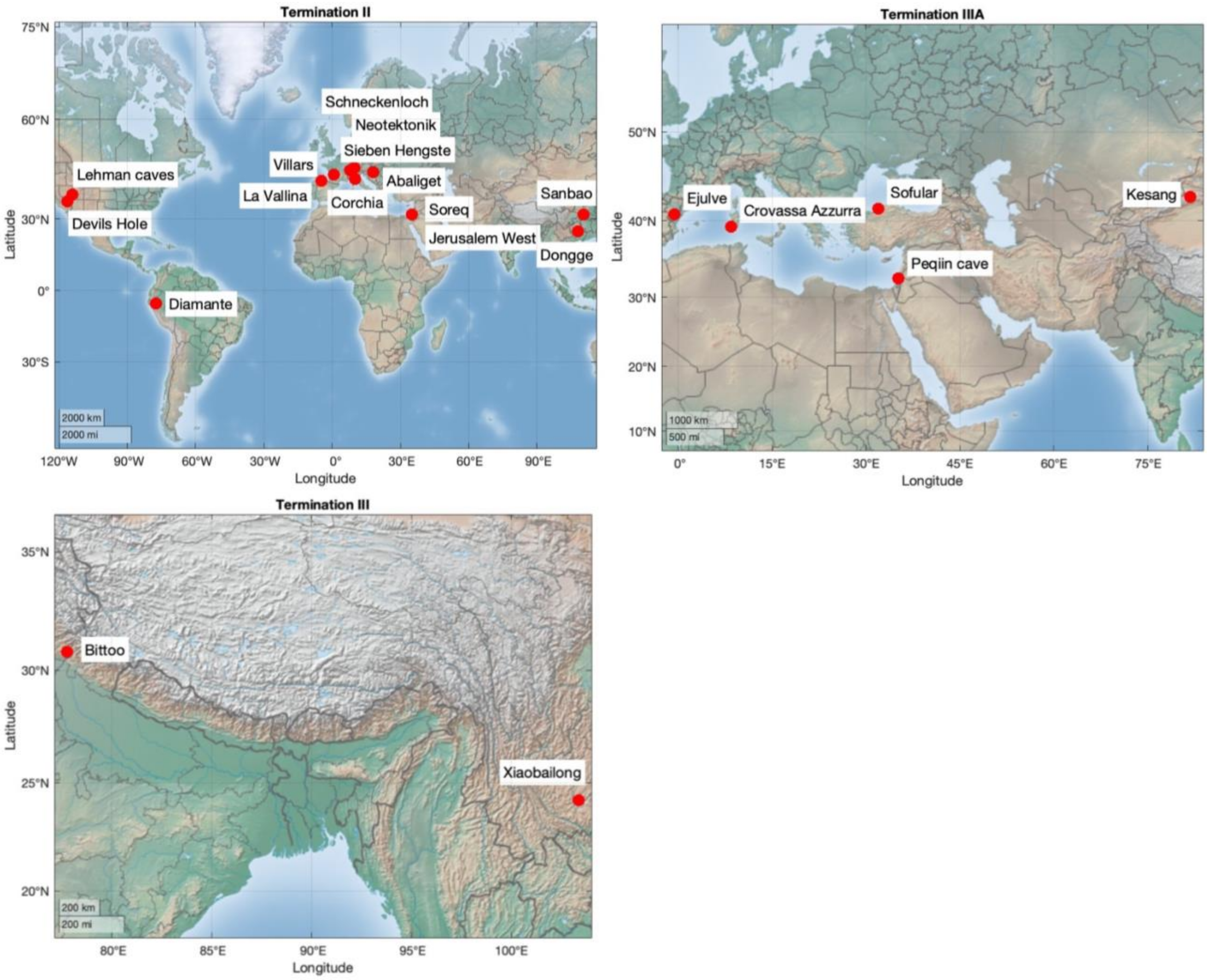

Supplementary figure 1: Maps plotting locations of speleothem entities that were not analysed as a part of the main manuscript since they only partially cover Terminations or have lower resolution or U-Th dates with larger errors than the records used in the main manuscript.

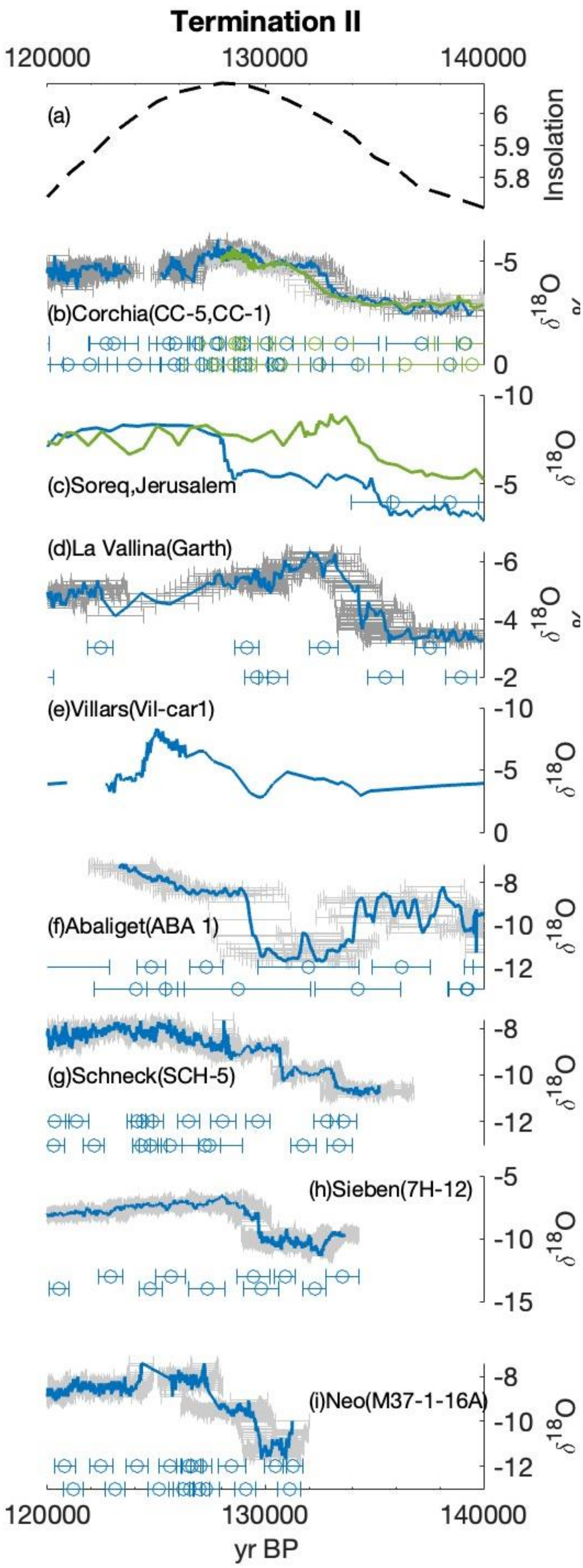
Termination II
120000
130000
140000
(a)
Insolation
6
5.9
5.8
(b)Corchia(CC-5,CC-1)
-5
0
(c)Soreq,Jerusalem
-10
-5
(d)La Vallina(Garth)
-6
-4
-2
(e)Villars(Vil-car1)
-10
-5
0
(f)Abaliget(ABA 1)
-8
-10
-12
(g)Schneck(SCH-5)
-8
-10
-12
(h)Sieben(7H-12)
-5
-10
-15
(i)Neo(M37-1-16A)
-8
-10
-12
$\delta^{18}O$
120000
130000
140000
yr BP

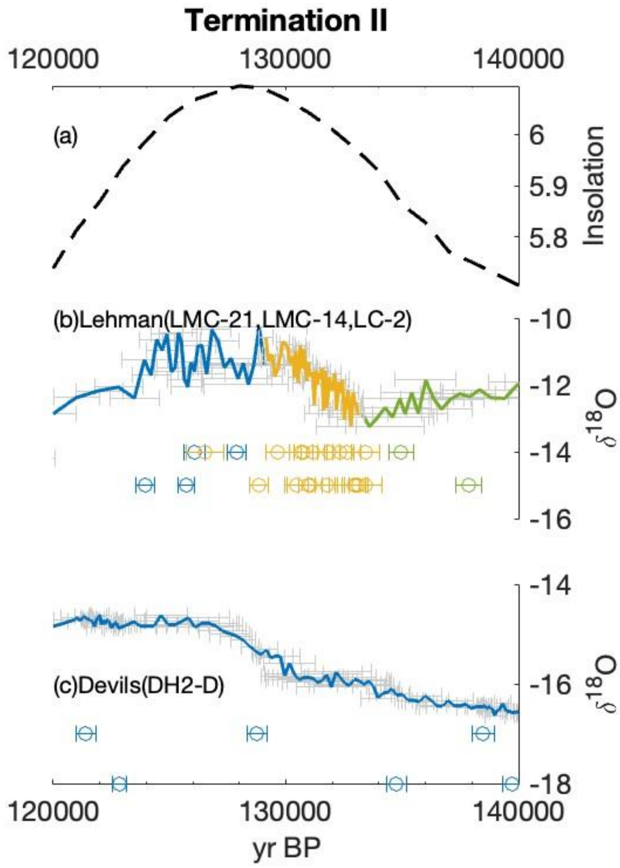
Termination II
120000
130000
140000
(a)
Insolation
6
5.9
5.8
(b)Lehman(LMC-21,LMC-14,LC-2)
-10
-12
-14
-16
(c)Devils(DH2-D)
-14
-16
-18
$\delta^{18}O$
120000
130000
140000
yr BP

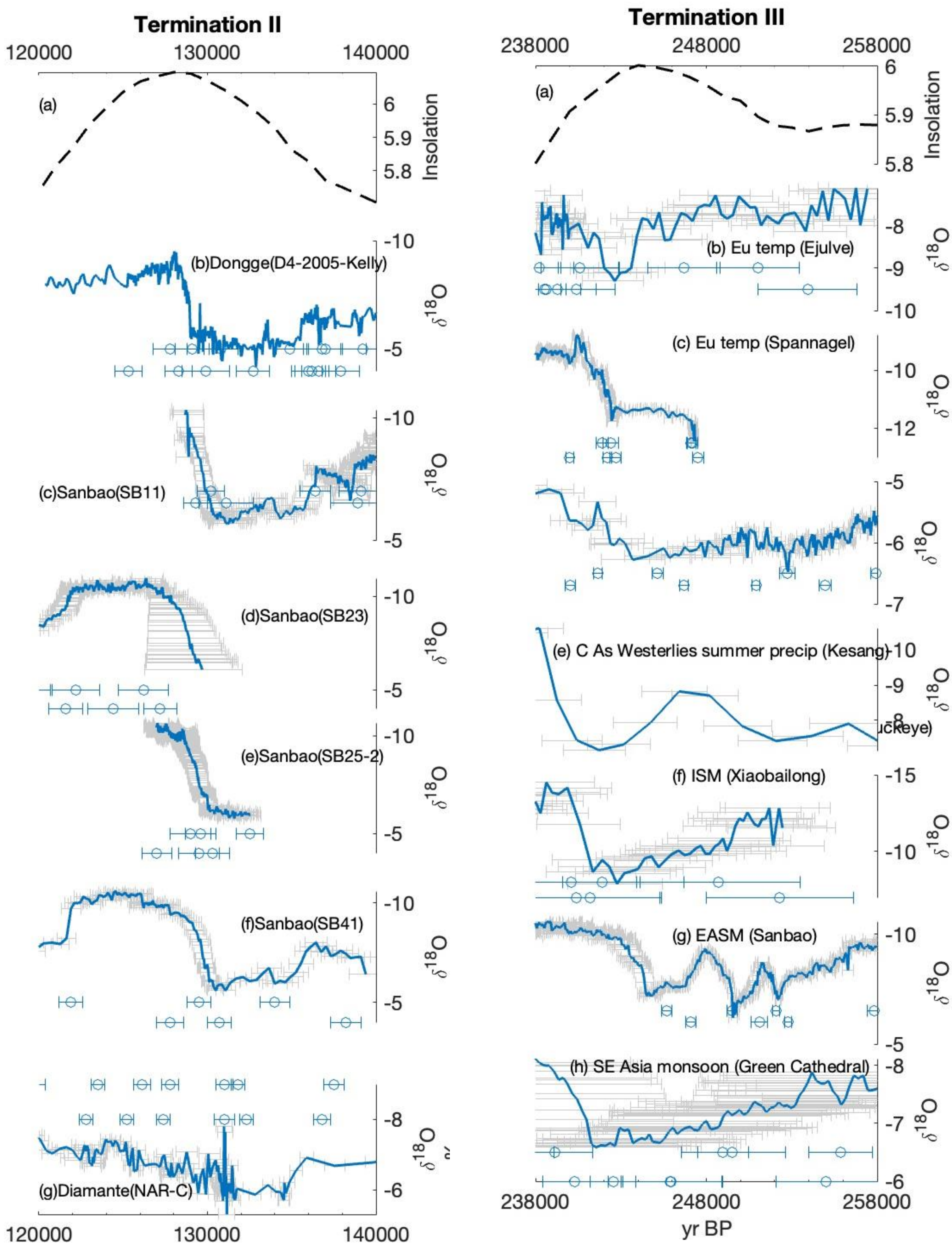

Supplementary figure 2: Plots of speleothem entities that were not analysed as a part of the main manuscript since they only partially cover Terminations or have lower resolution or U-Th dates with larger errors than the records used in the main manuscript. Key plots from the main manuscript have also been shown in these supplementary figures for comparison. Since a large number of records are available for Termination II, separate plot sections have been made for North Europe, North America and the monsoon records respectively. [precip = precipitation; temp = temperature; N Eu = North Europe; S Eu = South Europe; N Am = North America; C As = Central Asia; ISM = Indian Summer Monsoon; EASM = East Asian Summer Monsoon; SE Asia = Southeast Asia; S Am = South America]

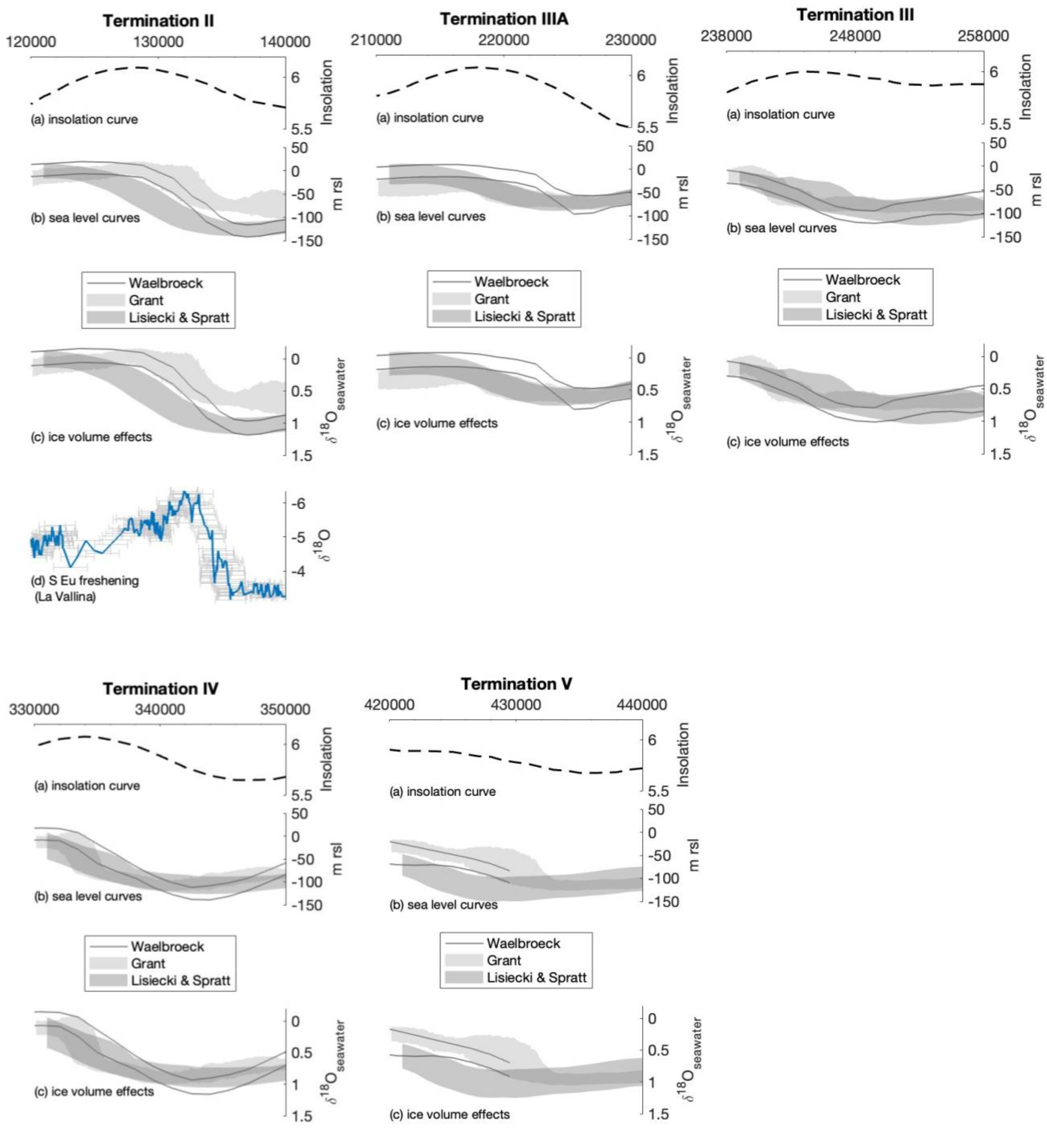

Supplementary figure 3: Ages covering Terminations are plotted against sea level curves and the ice volume effects on seawater oxygen isotopic records. Spratt and Lisiecki, Waelbroeck and Grant global sea level curves and linked-calculated ice volume effects on surface seawater $\delta^{18}O$ values are shown. For Termination II, the North Iberian Speleothem Archive (NISA) record is superimposed over the global curves to showcase the impact of regional North Atlantic changes in sea water $\delta^{18}O$ compared to the global curves. Insolation curve is the summer half year caloric insolation as provided in Tzedakis et al., 2017.

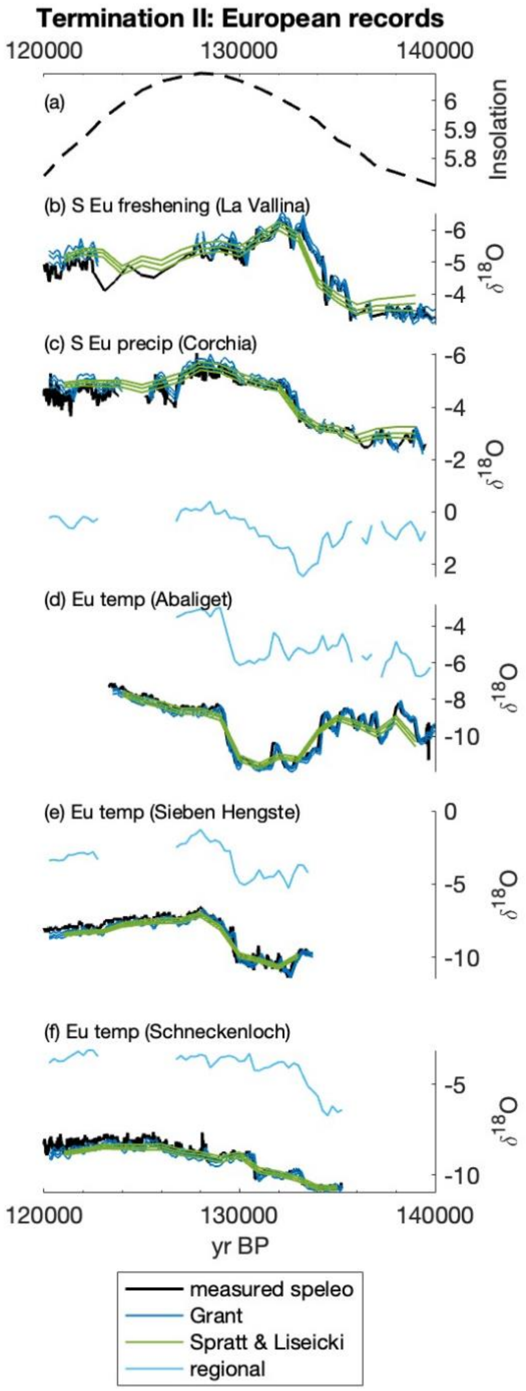
Termination II: European records
120000
130000
140000
(a)
6
5.9
5.8
Insolation
(b) S Eu freshening (La Vallina)
-6
-5
-4
δ18O
(c) S Eu precip (Corchia)
-6
-4
-2
0
2
δ18O
(d) Eu temp (Abaliget)
-4
-6
-8
-10
δ18O
(e) Eu temp (Sieben Hengste)
0
-5
-10
δ18O
(f) Eu temp (Schneckenloch)
-5
-10
δ18O
120000
130000
140000
yr BP
measured speleo
Grant
Spratt & Liseicki
regional

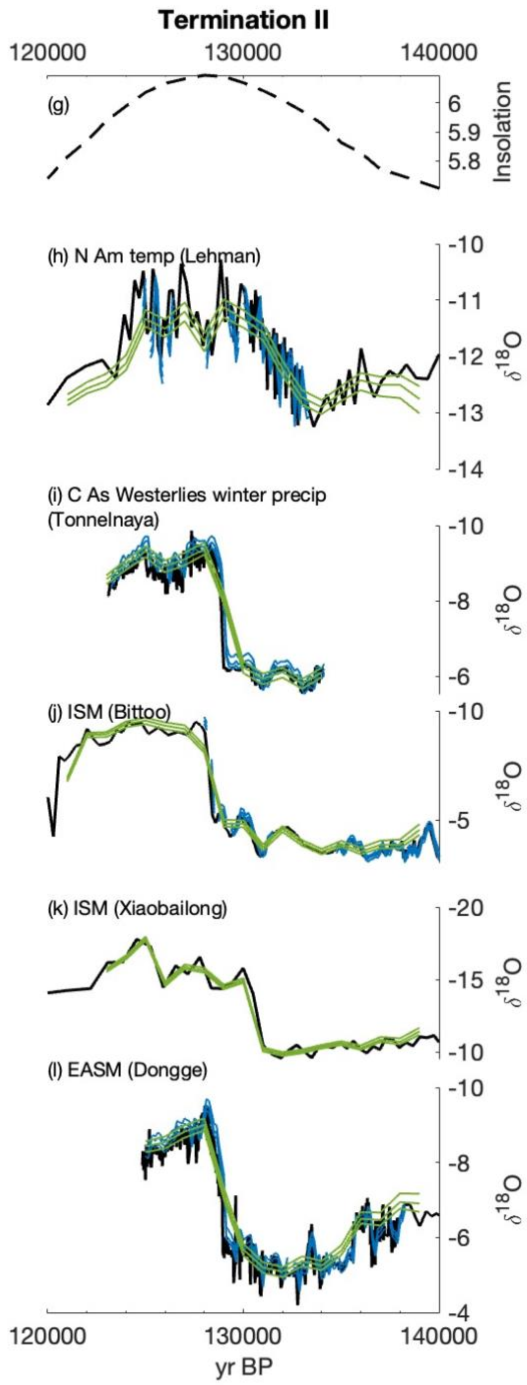
Termination II
120000
130000
140000
(g)
6
5.9
5.8
Insolation
(h) N Am temp (Lehman)
-10
-11
-12
-13
-14
δ18O
(i) C As Westerlies winter precip (Tonnelnaya)
-10
-8
-6
δ18O
(j) ISM (Bittoo)
-10
-5
δ18O
(k) ISM (Xiaobailong)
-20
-15
-10
δ18O
(l) EASM (Dongge)
-10
-8
-6
-4
δ18O
120000
130000
140000
yr BP

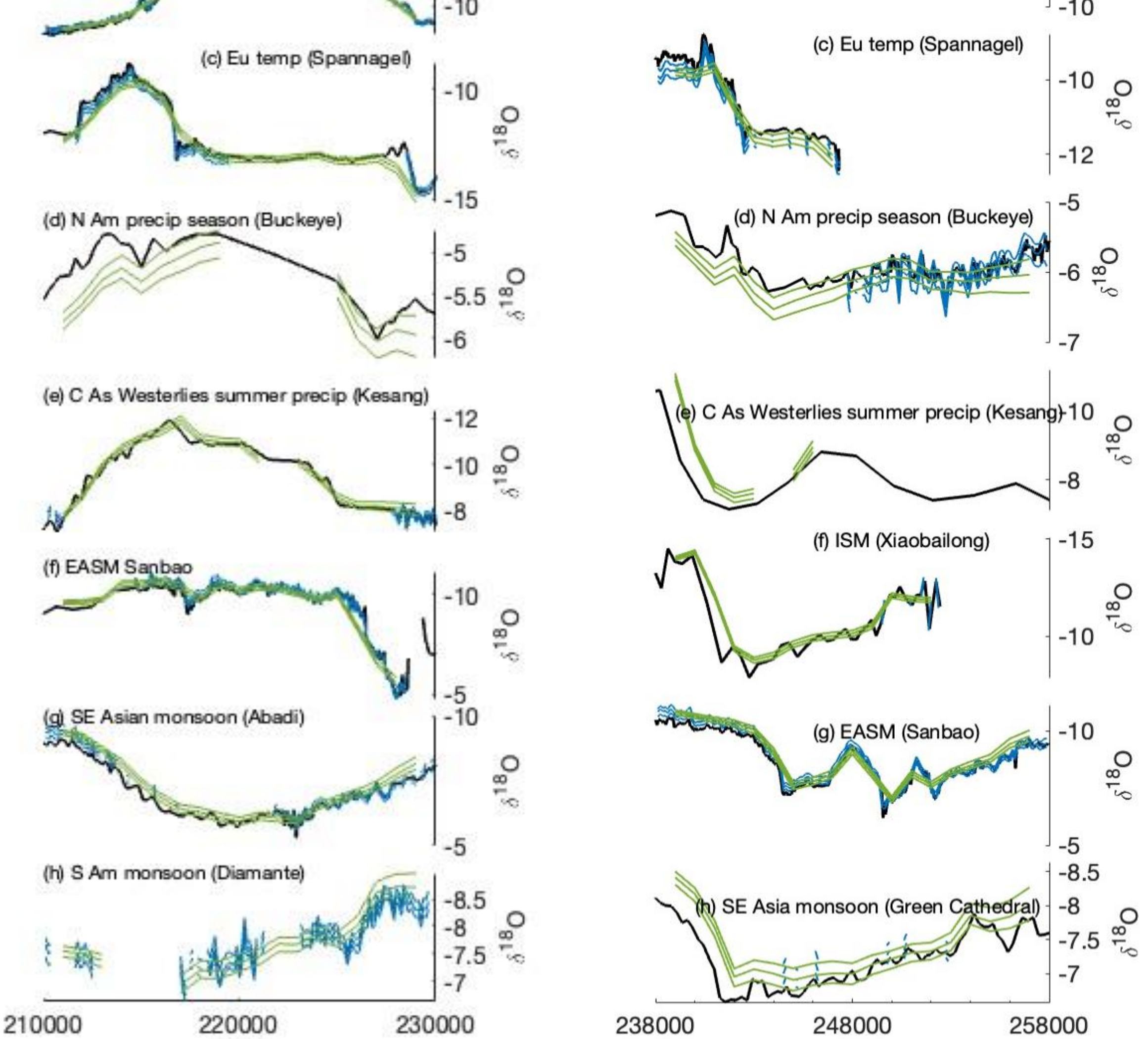

Termination IIIA
210000
220000
230000
(a)
6
5.5
Insolation
(b) Black Sea freshening (Sofular)
-20
-15
-10
δ18O
(c) Eu temp (Spannagel)
-10
-15
(d) N Am precip season (Buckeye)
-5
-5.5
-6
(e) C As Westerlies summer precip (Kesang)
-12
-10
-8
(f) EASM Sanbao
-10
-5
(g) SE Asian monsoon (Abadi)
-10
-5
(h) S Am monsoon (Diamante)
-8.5
-8
-7.5
-7
yr BP
Termination III
238000
248000
258000
(a)
6
5.9
5.8
Insolation
(b) Eu temp (Ejulve)
-8
-10
(c) Eu temp (Spannagel)
-10
-12
(d) N Am precip season (Buckeye)
-5
-6
-7
(e) C As Westerlies summer precip (Kesang)
-10
-8
(f) ISM (Xiaobailong)
-15
-10
(g) EASM (Sanbao)
-10
-5
(h) SE Asia monsoon (Green Cathedral)
-8.5
-8
-7.5
-7
yr BP

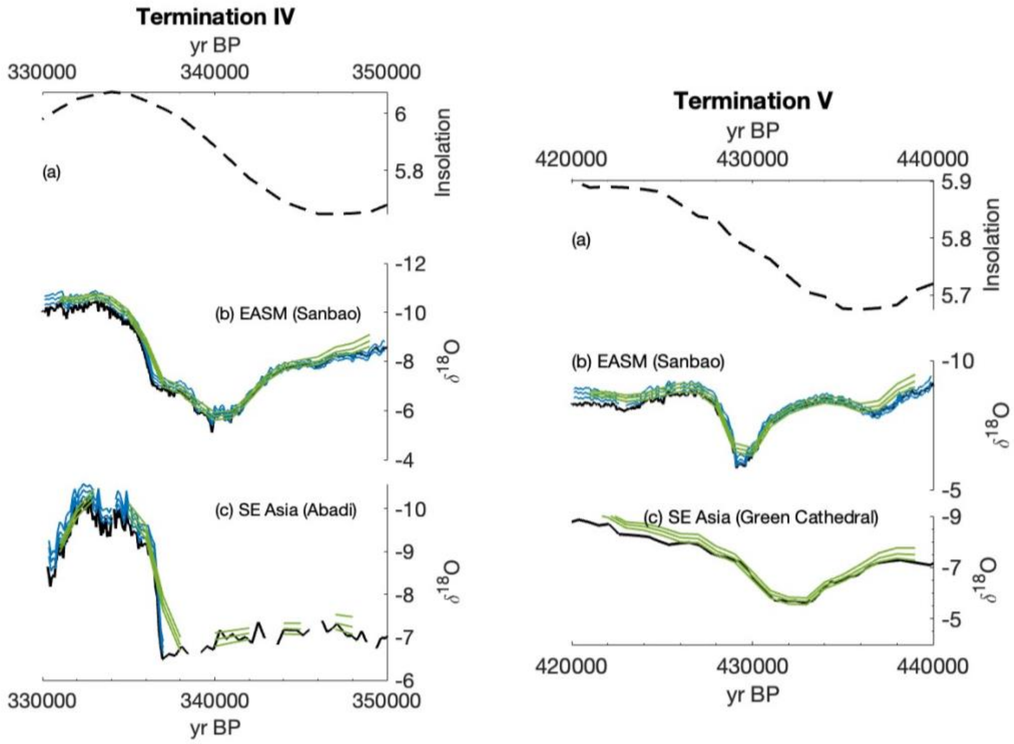

Supplementary figure 4: Ages covering Terminations are plotted against the ice volume effects on speleothem oxygen isotopic records. Spratt and Lisiecki and Grant ice volume effects are shown. For Termination II, the North Iberian Speleothem Archive (NISA) record is superimposed over the Europe speleothem data to showcase the impact of regional North Atlantic changes in sea water δ^{18}O compared to the global curves. Insolation curve is the summer half year caloric insolation as provided in Tzedakis et al., 2017. [precip = precipitation; temp = temperature; N Eu = North Europe; S Eu = South Europe; N Am = North America; C As = Central Asia; ISM = Indian Summer Monsoon; EASM = East Asian Summer Monsoon; SE Asia = Southeast Asia; S Am = South America]

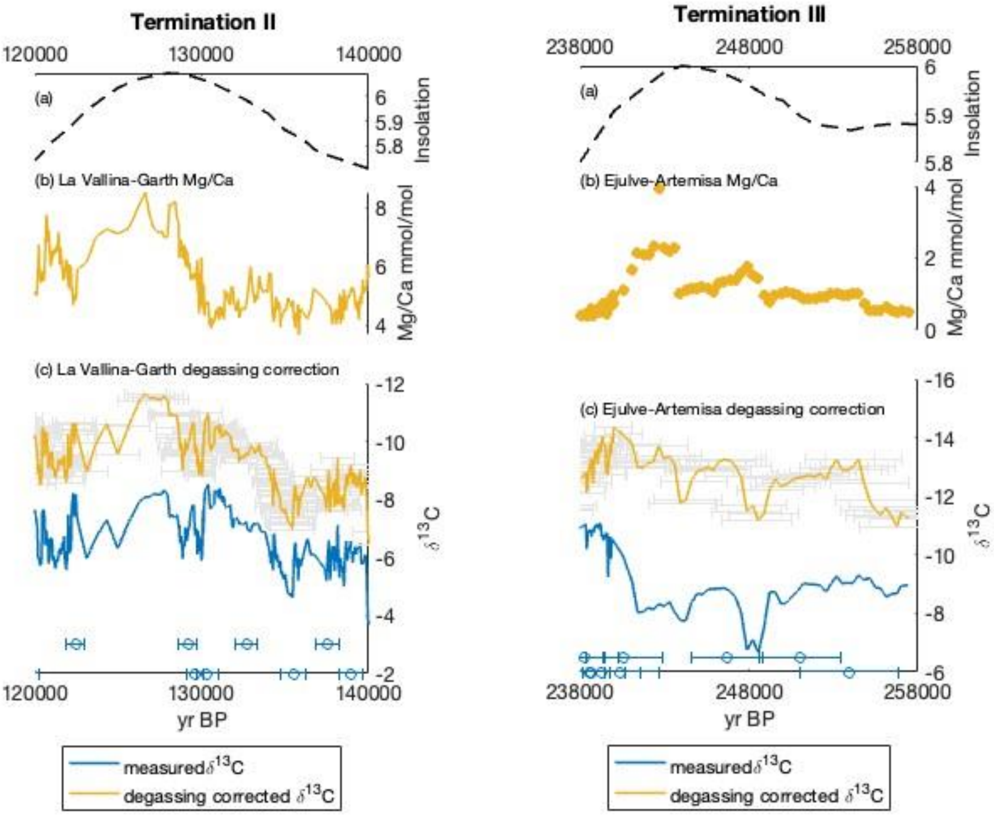

Supplementary figure 5: Ages covering Terminations for the South European records from La Vallina and Ejulve caves are plotted against measured δ^{13}C, degassing corrected δ^{13}C ($\delta^{13}C_{corr}$) and Mg/Ca records. The $\delta^{13}C_{corr}$ values are derived from an index based on the Mg/Ca data providing δ^{13}C 'initial' values that give temperature information.

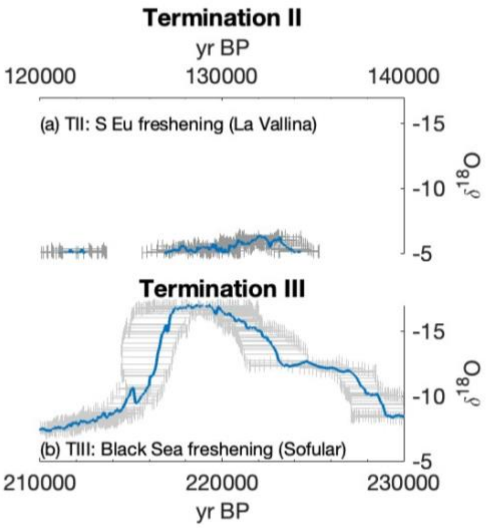

Supplementary figure 6: Ages covering Terminations are plotted against oxygen isotopic measurements. The Y-axis limits are constant across the sub-plots so that δ^{18}O anomaly magnitudes can be compared across different Terminations in speleothems encoding a similar climatic signal of surface ocean freshening. [S Eu = South Europe]

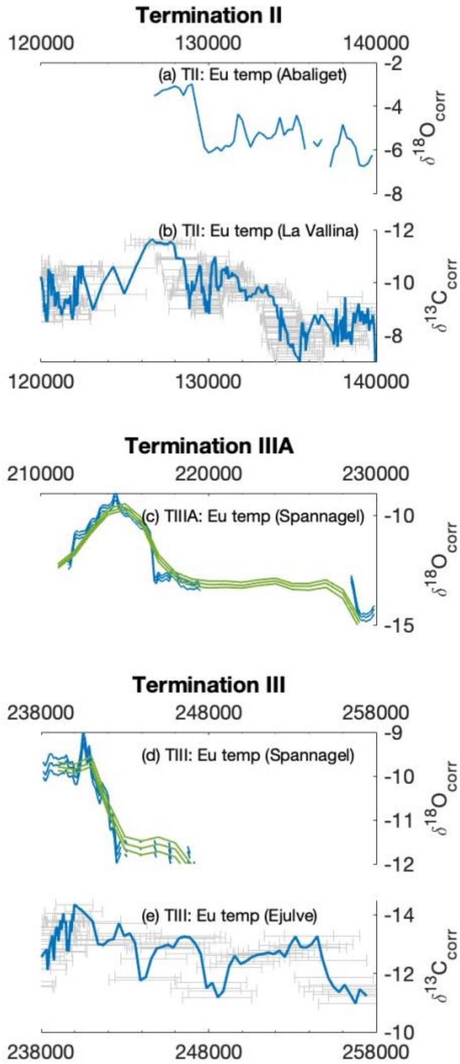

Supplementary figure 7: Ages covering Terminations are plotted against oxygen and carbon isotopic measurements. The records cover different Terminations encoding a similar climatic signal of temperature. [temp = temperature; Eu = Europe]

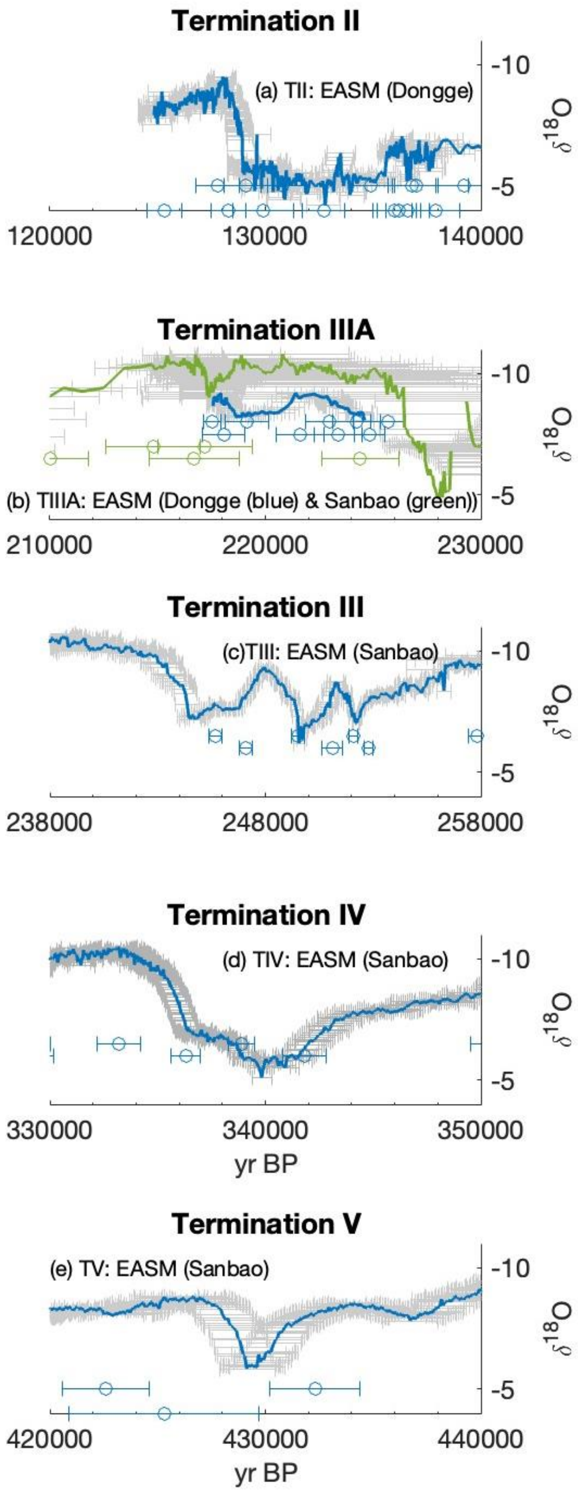
Termination II
(a) TII: EASM (Dongge)
-10
-5
δ18O
120000
130000
140000
Termination IIIA
(b) TIIIA: EASM (Dongge (blue) & Sanbao (green))
-10
-5
δ18O
210000
220000
230000
Termination III
(c)TIII: EASM (Sanbao)
-10
-5
δ18O
238000
248000
258000
Termination IV
(d) TIV: EASM (Sanbao)
-10
-5
δ18O
330000
340000
350000
yr BP
Termination V
(e) TV: EASM (Sanbao)
-10
-5
δ18O
420000
430000
440000
yr BP

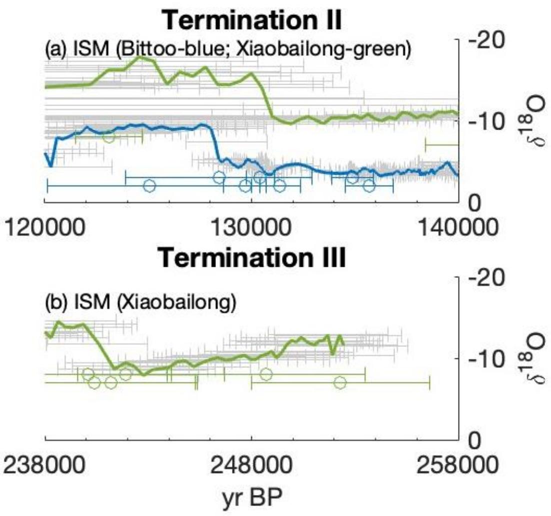
Termination II
(a) ISM (Bittoo-blue; Xiaobailong-green)
-20
-10
0
δ18O
120000
130000
140000
Termination III
(b) ISM (Xiaobailong)
-20
-10
0
δ18O
238000
248000
258000
yr BP

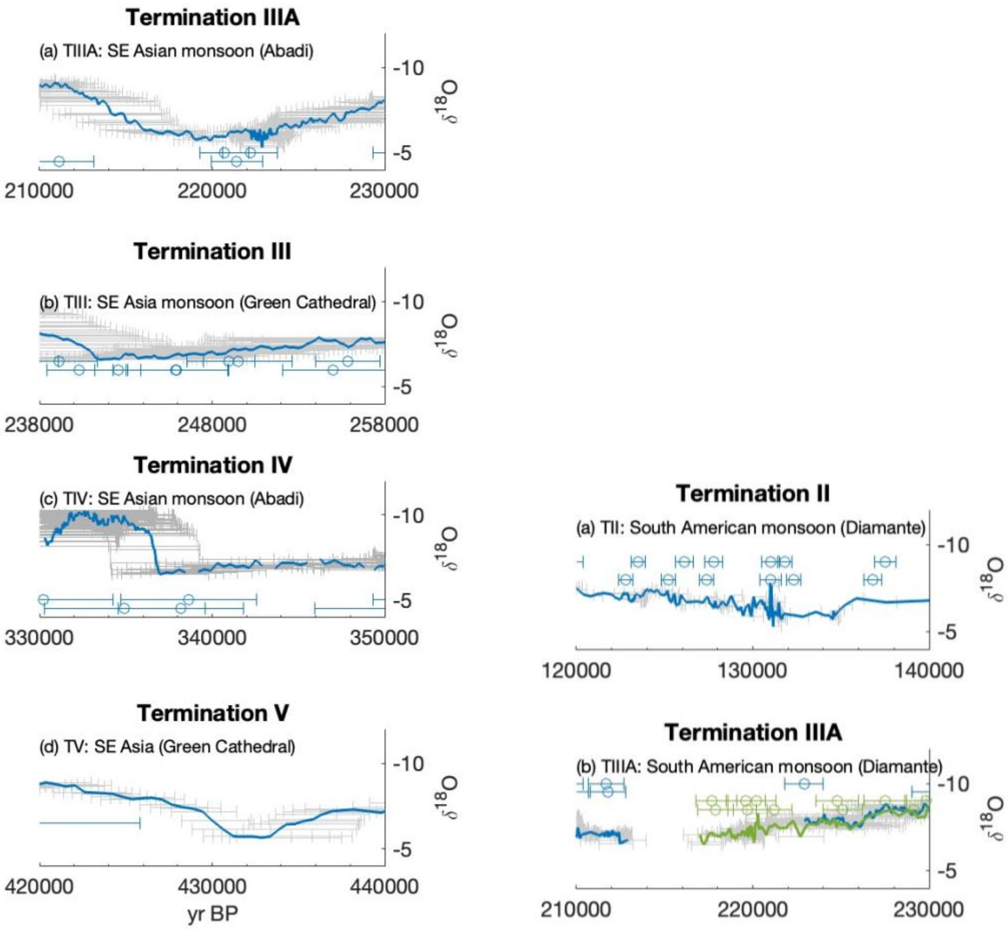

Supplementary figure 8: Ages covering Terminations are plotted against oxygen isotopic measurements. The Y-axis limits are constant across the sub-plots so that δ^{18}O anomaly magnitudes can be compared across different Terminations in speleothems encoding a similar climatic signal of monsoon-driven changes. [precip = precipitation; temp = temperature; N Eu = North Europe; S Eu = South Europe; N Am = North America; C As = Central Asia; ISM = Indian Summer Monsoon; EASM = East Asian Summer Monsoon; SE Asia = Southeast Asia; S Am = South America]

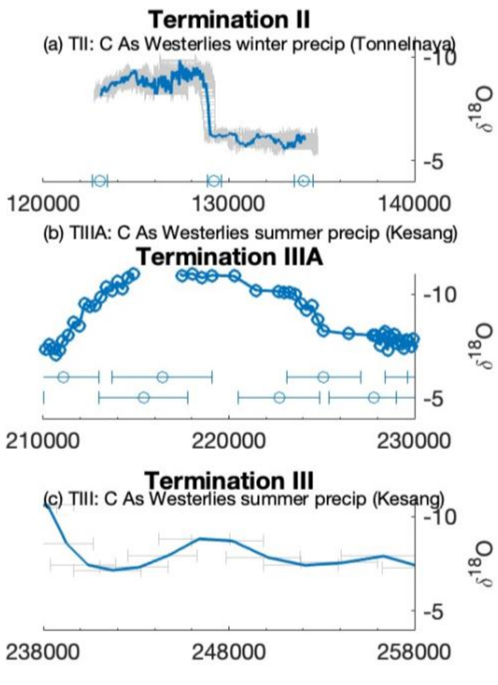

Supplementary figure 9: Ages covering Terminations are plotted against oxygen isotopic measurements. The Y-axis limits are constant across the sub-plots so that δ^{18}O anomaly magnitudes can be compared across different Terminations in speleothems encoding a similar climatic signal of Westerlies driven changes. [precip = precipitation; C As = Central Asia]

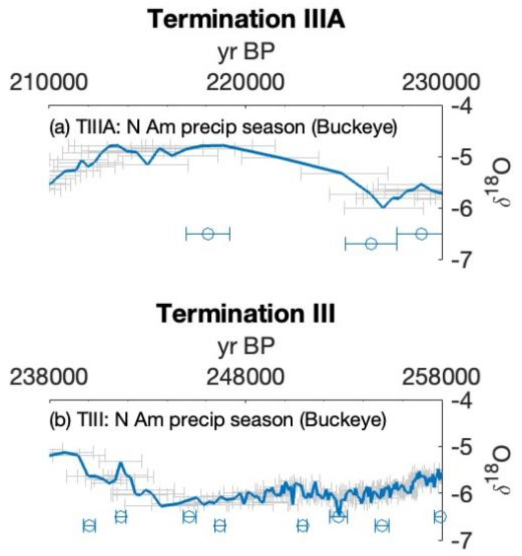

Supplementary figure 10: Ages covering Terminations are plotted against oxygen isotopic measurements. The Y-axis limits are constant across the sub-plots so that *δ*^{18}O anomaly magnitudes can be compared across different Terminations in speleothems encoding a similar climatic signal of source moisture and seasonality changes. [precip = precipitation; N Am = North America]

Badertscher, S., Fleitmann, D., Cheng, H., Edwards, R. L., Göktürk, O. M., Zumbühl, A., Leuenberger, M., and Tüysüz, O.: Pleistocene water intrusions from the Mediterranean and Caspian seas into the Black Sea, Nat. Geosci., 4, 236–239, https://doi.org/10.1038/ngeo1106, 2011.

Bar-Matthews, M., Ayalon, A., Gilmour, M., Matthews, A., and Hawkesworth, C. J.: Sea–land oxygen isotopic relationships from planktonic foraminifera and speleothems in the Eastern Mediterranean region and their implication for paleorainfall during interglacial intervals, Geochim. Cosmochim. Acta, 67, 3181–3199, https://doi.org/10.1016/S0016-7037(02)01031-1, 2003.

Cai, Y., Fung, I. Y., Edwards, R. L., An, Z., Cheng, H., Lee, J.-E., Tan, L., Shen, C.-C., Wang, X., Day, J. A., Zhou, W., Kelly, M. J., and Chiang, J. C. H.: Variability of stalagmite-inferred Indian monsoon precipitation over the past 252,000 y, Proc. Natl. Acad. Sci., 112, 2954–2959, https://doi.org/10.1073/pnas.1424035112, 2015.

Cheng, H., Spötl, C., Breitenbach, S. F. M., Sinha, A., Wassenburg, J. A., Jochum, K. P., Scholz, D., Li, X., Yi, L., Peng, Y., Lv, Y., Zhang, P., Votintseva, A., Loginov, V., Ning, Y., Kathayat, G., and Edwards, R. L.: Climate variations of Central Asia on orbital to millennial timescales, Sci. Rep., 6, 36975, https://doi.org/10.1038/srep36975, 2016a.

Cheng, H., Edwards, R. L., Sinha, A., Spötl, C., Yi, L., Chen, S., Kelly, M., Kathayat, G., Wang, X., Li, X., Kong, X., Wang, Y., Ning, Y., and Zhang, H.: The Asian monsoon over the past 640,000 years and ice age terminations, Nature, 534, 640–646, https://doi.org/10.1038/nature18591, 2016b.

Columbu, A., Spötl, C., De Waele, J., Yu, T.-L., Shen, C.-C., and Gázquez, F.: A long record of MIS 7 and MIS 5 climate and environment from a western Mediterranean speleothem (SW Sardinia, Italy), Quat. Sci. Rev., 220, 230–243, https://doi.org/10.1016/j.quascirev.2019.07.023, 2019.

Frumkin, A., Ford, D. C., and Schwarcz, H. P.: Continental Oxygen Isotopic Record of the Last 170,000 Years in Jerusalem, Quat. Res., 51, 317–327, https://doi.org/10.1006/qres.1998.2031, 1999.

Kathayat, G., Cheng, H., Sinha, A., Spötl, C., Edwards, R. L., Zhang, H., Li, X., Yi, L., Ning, Y., Cai, Y., Lui, W. L., and Breitenbach, S. F. M.: Indian monsoon variability on millennial-orbital timescales, Sci. Rep., 6, 24374, https://doi.org/10.1038/srep24374, 2016.

Kelly, M. J., Edwards, R. L., Cheng, H., Yuan, D., Cai, Y., Zhang, M., Lin, Y., and An, Z.: High resolution characterization of the Asian Monsoon between 146,000 and 99,000 years B.P. from Dongge Cave, China and global correlation of events surrounding Termination II, Palaeogeogr. Palaeoclimatol. Palaeoecol., 236, 20–38, https://doi.org/10.1016/j.palaeo.2005.11.042, 2006.

Koltai, G., Spötl, C., Shen, C.-C., Wu, C.-C., Rao, Z., Palcsu, L., Kele, S., Surányi, G., and Bárány-Kevei, I.: A penultimate glacial climate record from southern Hungary, J. Quat. Sci., 32, 946–956, https://doi.org/10.1002/jqs.2968, 2017.

Lachniet, M. S., Denniston, R. F., Asmerom, Y., and Polyak, V. J.: Orbital control of western North America atmospheric circulation and climate over two glacial cycles, Nat. Commun., 5, 3805, https://doi.org/10.1038/ncomms4805, 2014.

Luetscher, M., Moseley, G. E., Festi, D., Hof, F., Edwards, R. L., and Spötl, C.: A Last Interglacial speleothem record from the Sieben Hengste cave system (Switzerland): Implications for alpine paleovegetation, Quat. Sci. Rev., 262, 106974, https://doi.org/10.1016/j.quascirev.2021.106974, 2021.

Moseley, G. E., Spötl, C., Cheng, H., Boch, R., Min, A., and Edwards, R. L.: Termination-II interstadial/stadial climate change recorded in two stalagmites from the north European Alps, Quat. Sci. Rev., 127, 229–239, https://doi.org/10.1016/j.quascirev.2015.07.012, 2015.

Moseley, G. E., Edwards, R. L., Wendt, K. A., Cheng, H., Dublyansky, Y., Lu, Y., Boch, R., and Spötl, C.: Reconciliation of the Devils Hole climate record with orbital forcing, Science, 351, 165–168, https://doi.org/10.1126/science.aad4132, 2016.

Pérez-Mejías, C., Moreno, A., Sancho, C., Bartolomé, M., Stoll, H., Cacho, I., Cheng, H., and Edwards, R. L.: Abrupt climate changes during Termination III in Southern Europe, Proc. Natl. Acad. Sci., 114, 10047–10052, https://doi.org/10.1073/pnas.1619615114, 2017.

Shakun, J. D., Burns, S. J., Clark, P. U., Cheng, H., and Edwards, R. L.: Milankovitch-paced Termination II in a Nevada speleothem?, Geophys. Res. Lett., 38, https://doi.org/10.1029/2011GL048560, 2011.

Stoll, H. M., Cacho, I., Gasson, E., Sliwinski, J., Kost, O., Moreno, A., Iglesias, M., Torner, J., Perez-Mejias, C., Haghipour, N., Cheng, H., and Edwards, R. L.: Rapid northern hemisphere ice sheet melting during the penultimate deglaciation, Nat. Commun., 13, 3819, https://doi.org/10.1038/s41467-022-31619-3, 2022.

Tzedakis, P. C., Crucifix, M., Mitsui, T., and Wolff, E. W.: A simple rule to determine which insolation cycles lead to interglacials, Nature, 542, 427–432, https://doi.org/10.1038/nature21364, 2017.

Tzedakis, P. C., Drysdale, R. N., Margari, V., Skinner, L. C., Menviel, L., Rhodes, R. H., Taschetto, A. S., Hodell, D. A., Crowhurst, S. J., Hellstrom, J. C., Fallick, A. E., Grimalt, J. O., McManus, J. F., Martrat, B., Mokeddem, Z., Parrenin, F., Regattieri, E., Roe, K., and Zanchetta, G.: Enhanced climate instability in the North Atlantic and southern Europe during the Last Interglacial, Nat. Commun., 9, 4235, https://doi.org/10.1038/s41467-018-06683-3, 2018.

Wainer, K., Genty, D., Blamart, D., Daëron, M., Bar-Matthews, M., Vonhof, H., Dublyansky, Y., Pons-Branchu, E., Thomas, L., van Calsteren, P., Quinif, Y., and Caillon, N.: Speleothem record of the last 180 ka in Villars cave (SW France): Investigation of a large δ18O shift between MIS6 and MIS5, Quat. Sci. Rev., 30, 130–146, https://doi.org/10.1016/j.quascirev.2010.07.004, 2011.

Wilcox, P. S., Honiat, C., Trüssel, M., Edwards, R. L., and Spötl, C.: Exceptional warmth and climate instability occurred in the European Alps during the Last Interglacial period, Commun. Earth Environ., 1, 1–6, https://doi.org/10.1038/s43247-020-00063-w, 2020.